Available online at www.sciencedirect.com
SCIENCE DIRECT
Fluid Phase Equilibria 230 (2005) 72–80
FLUID PHASE EQUILIBRIA
www.elsevier.com/locate/fluid

High pressure (solid + liquid) equilibria of *n*-alkane mixtures: experimental results, correlation and prediction

Piotr Morawski[a], João A.P. Coutinho[b], Urszula Domańska[a,*]

[a] *Physical Chemistry Division, Faculty of Chemistry, Warsaw University of Technology, Noakowskiego 3, 00-664 Warsaw, Poland*
[b] *CICECO, Department of Chemistry, University of Aveiro, 3810-193 Aveiro, Portugal*

Received 13 August 2004; received in revised form 20 November 2004; accepted 22 November 2004
Available online 19 January 2005

Abstract

(Solid + liquid) equilibria (SLE) of {*n*-alkanes (*n*-tridecane, *n*-hexadecane, *n*-octadecane) + *n*-hexane} at very high pressures up to about 1.0 GPa have been investigated in the temperature range from 293 to 363 K using a thermostated apparatus for the measurements of transition pressures from the liquid to the solid state in two component isothermal solutions.

The polynomial based on the general solubility equation at atmospheric pressure was satisfactorily used to the description of the pressure-temperature-composition relation of the high pressure (solid + liquid) equilibria. Additionally, the SLE of the binary system (*n*-tridecane + *n*-hexane) at normal pressure was measured by the dynamic method. The results at higher pressures for every system were compared to those at normal pressure.

The main aim of this work was to predict the SLE of the mixtures using only pure components data in a wide pressure range, far above the pressure range in which cubic equations of state are normally applied. The fluid phase is described by the corrected SRK-EOS using van der Waals one fluid mixing rules. The results of the predictions are compared with the experimental data presented in this paper {*n*-alkanes (*n*-tridecane, *n*-hexadecane, *n*-octadecane) + *n*-hexane} and with experimental results presented previously {*n*-alkanes (*n*-tridecane, *n*-hexadecane, *n*-octadecane and *n*-eicosane) + cyclohexane}.

Keywords: (Solid + liquid) equilibria; *n*-Alkanes; Cyclohexane; *n*-Hexane; High-pressure; Correlation; Prediction; Modelling

1. Introduction

(Solid + liquid) equilibria (SLE) of *n*-alkanes systems have gained increasing interest in the recent decade. Besides its importance for crystallization and purification in fat, cosmetic and oil technology, SLE provide a good tool to study the thermodynamic nature of many systems and to test models. High-pressure data may be used in new high-pressure technology, which is a rapidly developing field nowadays. Phase equilibrium data of *n*-alkane systems are of importance for the safe and efficient operation of chemical plants. They are important for high-pressure polymerization processes and for oil-recovery processes.

From a historical perspective, the very first (solid + liquid) equilibria measurements of organic liquids at higher pressures was presented by Baranowski and Co-workers [1–4]. Simultaneously, results for different organic mixtures were presented by Nagaoka and Makita, [5–7], Nagaoka et al. [8] and Tanaka and Kawakami [9]. Recently, Yang et al. presented results involving *n*-alkane mixtures with alcohols [10,11]. The pressure effect on the phase behavior of binary mixtures of fatty acids up to 200 MPa was measured and well described by Inoue et al. [12]. In some papers different authors described (solid + liquid) equilibrium under high-pressure using the Chain Delta Lattice Parameter Model [13], the Sako-Wu-Prausnitz EOS (SWP) [14,15], or the van der Waals EOS [16]. Prediction of solid–fluid phase diagrams of light gases–heavy hydrocarbons systems up to 200 MPa using an equation of state

* Corresponding author. Tel.: +48 226 213115; fax: +48 226 282741.
E-mail address: ula@ch.pw.edu.pl (U. Domańska).

0378-3812/$ – see front matter © 2004 Elsevier B.V. All rights reserved.
doi:10.1016/j.fluid.2004.11.020

G^E model is developed and presented by Pauly et al. [17,18].

Mainly simple eutectic mixtures with complete miscibility in the liquid phase and immiscibility in the solid phase were tested in a wide temperature range from 243 to 373 K, i.e., the binary system (benzene + tiophene) [8]. SLE of binary mixtures were measured by an optical method from 278 to 343 K, and pressures up to 500 MPa for the organic systems: (benzene + 2-methyl-2-propanol) [5], (carbon tetrachloride + *p*-xylene, or benzene) [6], and (α-methylnaphthalene + β-methylnaphthalene) [7]. The eutectic mixtures become richer in the component with the highest slope d*p*/d*T* of the melting curve and the eutectic temperature rises with increasing pressure; also different compositions of the eutectic point are observed [6,7]. It is expected as well that at higher pressure the melting temperature of congruently melting compound increases or the nature of congruently/incongruently melting compound may change, what was observed for (carbon tetrachloride + benzene) system [6]. The solid system (chlorobenzene + bromobenzene) shows complete miscibility in the solid phase [8]. The first results for binary mixtures of *n*-alkanes were presented for the eutectic mixtures of (tetradecane, or hexadecane + cyclohexane, or benzene) at higher pressures, up to 120 MPa by Tanaka and Kawakami [9]. The SLE coexistence curve and the eutectic point shift to higher temperatures with an increase of pressure. Changing the pressure from 0.1 to 120 MPa increases the temperature of eutectic point for (tetradecane, or hexadecane + benzene) by 25 and 30 K, respectively. For the (tetradecane, or hexadecane + cyclohexane) binary system, the change of eutectic temperature is 30 and 35 K. The composition of the eutectic point shifts to higher concentration of the *n*-alkane. The pressure dependence of the solubilities of anthracene and phenanthrene in water shows a decrease of the partial molar volumes of these solutes in water with increasing pressure up to 200 MPa, as was shown recently [19].

In this paper, we present results obtained with a piston–cylinder apparatus [20,21] for three *n*-alkanes: (*n*-tridecane or *n*-hexadecane or *n*-octadecane + *n*-hexane). The data were measured at very high-pressure, up to 1.0 GPa, and in a wide temperature range, from 293 to 363 K. The experimental data will be described using the predictive method proposed by Pauly et al. [18] corrected in this paper for improved description of the phase behavior at very high pressures. The performance of the modified model is also tested using our data for (*n*-alkanes + cyclohexane), published previously [20]. The solid–liquid coexistence curves of these systems were also correlated by the equation proposed by Yang et al. [10,11].

2. Experimental

2.1. Materials

The origin of the chemicals is: *n*-tridecane (Koch-Light Lab.), *n*-hexadecane (International Enzymes Ltd., UK), *n*-octadecane (Koch-Light Lab.), *n*-hexane (Merck). The purity of *n*-alkanes was better than 99 mass% and they were used directly, without further purification. The physical properties of the pure *n*-alkanes used in the calculations are collected in Table 1.

2.2. Procedures

(Solid + liquid) equilibrium data of the system (tridecane + *n*-hexane) at 0.1 MPa were determined using a dynamic (synthetic) method, described in detail previously [25,26]. The thermometer was calibrated on the basis of the ITS-90 temperature scale. The accuracy of temperature measurements was ±0.01 K while the error in the mole fraction did not exceed $\delta x_1 = 0.0005$. The results are shown in Table 2 as x_1, the mole fraction of *n*-tridecane in the saturated solution (α or β crystalline forms of *n*-tridecane) as a function of T_1, the liquidus of *n*-tridecane-binary solution equilibrium. High pressure (solid + liquid) equilibria was measured with a simple piston–cylinder device, shown in Fig. 1. Apparatus was presented in detail in our previous papers [20,21]. The mobile piston (1) was moved by a hydraulic press. The mechanical indicator (11) monitored the displacement of the piston with an accuracy of 0.01 mm. Resistance was measured by a calibrated manganine gauge (8) connected to a digital multimeter

Table 1
Physical constants of pure compounds

Compound	$T_{fus,1}$ (K)	$\Delta_{fus}H_1$ (J mol^{-1})	$T_{tr,1}$[a] (K)	$\Delta^l_s Cp_m$ (J mol^{-1} K^{-1})	$\Delta_{tr}H_1$[a] (J mol^{-1})	T_{cr} (K)	P_{cr} (bar)	ω
n-Tridecane	267.6[b]	28485[b]	255	−105.94[b]	9162	676	17.0	0.622
n-Hexadecane	291.2[b]	53332[b]		77.68[b]		717	14.0	0.775
n-Octadecane	301.2[b]	61306[b]		80.84[b]		745	11.9	0.801
n-Eicosane	309.5[c]	69730[c]		54.00[c]		767	11.0	0.907
Cyclohexane	279.8[b]	2630[b]		14.63[b]		553	40.3	0.214
n-Hexane	177.8[b]	13124[b]		44.12[b]		508	30.3	0.299

Melting point, $T_{fus,1}$, solid–solid phase transition temperature, $T_{tr,1}$, molar enthalpy $\Delta_{fus}H_1$ of fusion, molar enthalpy of transition, $\Delta_{tr}H_1$, heat capacity of transition $\Delta^l_s Cp_m$, critical temperature T_{cr}, critical pressure P_{cr}, acentric factor ω.

[a] Ref. [22].

[b] Ref. [23].

[c] Ref. [24].

Table 2
Experimental (solid + liquid) equilibria temperatures of {*n*-tridecane (1) + *n*-hexane (2)} system at 0.1 MPa

x_1	$T_{1\alpha}$ (K)	x_1	$T_{1\alpha}$ (K)	x_1	$T_{1\beta}$ (K)
1.0000	268.21	0.6784	262.12	0.4328	253.11
0.9876	268.02	0.6512	261.27	0.4119	252.25
0.9782	267.97	0.6301	260.38	0.3777	250.93
0.9599	267.75	0.6116	259.46	0.3251	249.47
0.9357	267.18	0.5919	259.30	0.3033	248.92
0.9034	266.84	0.5752	259.16	0.2786	247.95
0.8730	266.43	0.5564	258.86	0.2229	244.99
0.8496	265.62	0.5147	257.95	0.2048	244.05
0.8284	264.79	0.4685	255.18	0.1603	240.89
0.8008	264.39			0.1331	238.66
0.7786	264.11			0.1157	236.78
0.7597	263.16			0.0676	229.59
0.7378	262.85			0.0443	226.21
0.7225	262.73			0.0341	224.18
0.7036	262.31			0.0263	218.86

T_1: liquidus for α and β crystalline forms of *n*-tridecane.

Hewlett-Packard 3478A (10) with an accuracy of ±0.001 Ω. The device was thermostated with water thermostat, and the temperature was measured by a Pt-resistance thermometer Delta HD 9215 (Poland) with an accuracy of ±0.1 K. Temperature was controlled by a thermocouple (7). The pressure was measured up to 1.0 GPa with an error of ±2%. Liquid–solid phase transitions were determined by sharp discontinuities of volume–pressure curves. The accuracy of the discontinuity in *P–V* curves is assumed to be ±2% of the pressure. The initiation of freezing was noticed at a higher pressure than the equilibrium value of this phase transition, observed as an "overpressure" effect (the intersection between the lines of the one- and two-phase regions). The results published are the average of three or more measurements at the intersection point. The final equilibrium point is the first point

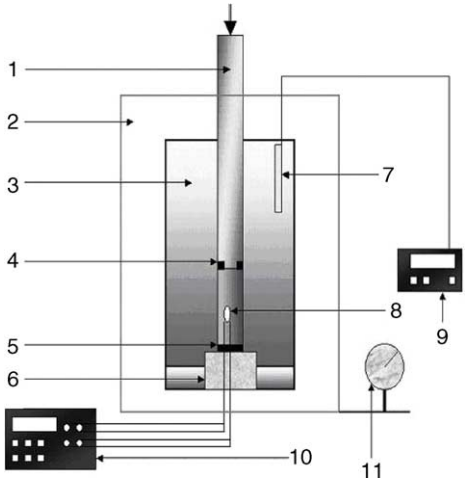

Fig. 1. Scheme of the high-pressure device: (1) piston; (2) thermstate; (3) steel vessel; (4,5) metallic rings; (6) high-pressure stopper with wires; (7) Pt(1 0 0) thermocouple; (8) manganine gauge; (9) digital thermometer; (10) digital multimeter; (11) mechanical indicator of position.

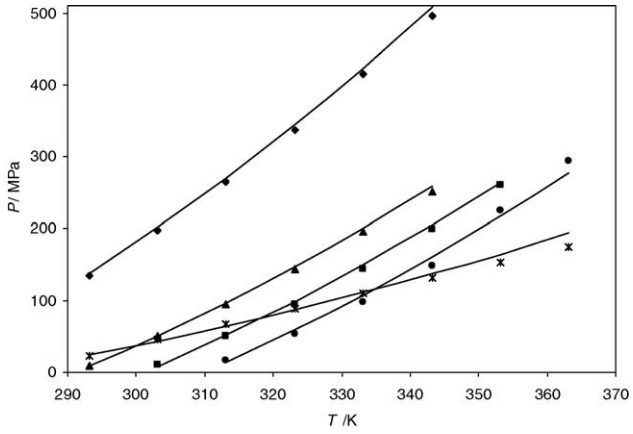

Fig. 2. Modelling of pure components data using the predictive method proposed on this work (Eq. (11)). (♦) *n*-tridecane, (▲) *n*-hexadecane, (■) *n*-octadecane, (●) *n*-eicosane, (✖) cyclohexane, (—) prediction.

of the second line of the equilibrium noted for the solid phase.

3. Results and discussion

(Solid + liquid) equilibria of the systems (*n*-hexadecane, or *n*-octadecane + *n*-hexane) at atmospheric pressure were measured previously [25,26]. For crystals with simple structures, the pressure dependence of the melting point can be described with the semi-empirical equation of Simon [27], as was done earlier [20]. The behavior of the pure substances can be also purely predicted with very good accuracy using the model described in this paper as is shown in Fig. 2.

The effect of pressure on the (solid + liquid) phase equilibria of the binary mixtures has been measured at various constant compositions and temperatures. The liquid–solid transitions were determined for the whole *n*-alkane concentration

Table 3
Experimental pressures *P* and compositions of *n*-tridecane, x_1 for the {*n*-tridecane (1) + *n*-hexane (2)} systems at constant temperatures *T*

x_1	*T* (K)					
	293.15	303.15	313.15	323.15	333.15	343.15
P (MPa)						
1.0000	133.01	197.12	265.40	337.83	414.42	495.17
0.9237	142.51	207.56	275.95	348.91	425.71	504.09
0.8587	152.47	218.84	286.50	360.21	437.53	513.02
0.8156	157.63	224.74	294.33	366.40	440.94	517.96
0.7359	170.01	237.37	307.52	378.46	452.97	529.98
0.6708	182.40	250.00	320.71	390.52	465.00	542.00
0.5789	197.36	266.72	339.46	415.58	495.06	577.92
0.5006	217.26	285.96	360.20	439.96	525.25	616.07
0.4256	237.16	305.20	380.93	464.34	555.44	654.21
0.3158	269.68	347.87	431.32	520.03	619.72	728.11
0.2442	302.20	390.54	481.71	575.72	684.27	802.10
0.1777	335.11	441.00	533.50	639.36	756.22	891.78
0.1372	364.08	473.70	578.92	693.74	818.03	968.21
0.0806	395.22	510.35	626.01	756.84	895.35	1059.44
0.0232	436.17	547.00	675.17	820.69	983.54	1163.74

Table 4
Experimental pressures P and compositions of the n-hexadecane, x_1 for the {n-hexadecane (1) + n-hexane (2)} systems at constant temperatures T

x_1	T (K)					
	293.15	303.15	313.15	323.15	333.15	343.15
P (MPa)						
1.0000	9.21	50.65	95.56	143.92	195.74	251.03
0.9543	10.67	54.88	102.17	149.52	201.95	257.44
0.8885	12.12	59.11	108.78	161.13	216.15	273.85
0.8316	13.49	61.70	112.88	167.02	224.11	284.15
0.7845	14.85	64.30	116.98	172.90	232.06	294.46
0.6955	25.31	75.41	128.74	185.29	245.07	308.08
0.6002	35.77	86.53	140.50	197.68	258.09	321.71
0.5026	41.44	92.58	150.58	212.44	277.17	344.75
0.3674	55.10	116.63	180.67	247.20	316.24	387.79
0.2765	91.90	151.10	215.21	284.23	358.15	436.97
0.2007	128.70	185.58	249.76	321.26	400.05	486.16
0.1000	204.71	270.17	346.02	432.26	528.89	635.91
0.0260	469.45	548.68	645.85	760.97	894.02	1045.01

Table 5
Experimental pressures P and compositions of n-octadecane, x_1 for the {n-octadecane (1) + n-hexane (2)} systems at constant temperatures T

x_1	T (K)					
	293.15	303.15	313.15	323.15	333.15	343.15
P (MPa)						
1.0000	8.86	49.60	94.90	144.78	199.22	258.23
0.9401	12.04	55.67	102.98	153.97	208.63	266.97
0.8673	15.22	61.74	111.05	163.16	218.04	275.72
0.8193	19.13	64.92	114.14	166.78	222.84	282.33
0.7785	23.05	68.10	117.22	170.40	227.63	288.93
0.6997	35.02	77.15	124.64	177.50	235.74	299.34
0.6200	47.00	86.19	132.06	184.61	243.84	309.74
0.5344	53.94	97.57	146.42	200.51	259.82	324.36
0.4590	60.89	108.94	160.78	216.40	275.80	338.98
0.3865	70.74	121.96	176.99	235.82	298.45	364.88
0.3210	80.59	134.98	193.20	255.23	321.09	390.77
0.2509	97.98	156.29	217.79	282.49	350.37	421.44
0.1986	115.37	177.60	242.39	309.74	379.65	452.12
0.1066	176.98	241.66	312.77	390.34	474.35	564.81
0.0608	238.60	305.71	383.16	470.94	569.05	677.49

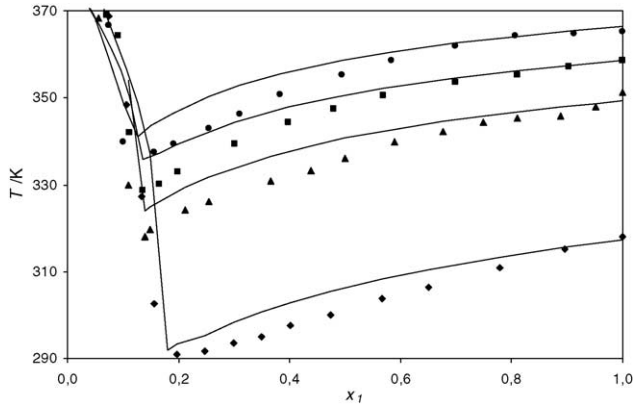

Fig. 3. Prediction of freezing temperatures (within the range of experimental temperature) of systems {n-alkane (1) + cyclohexane (2)} at the pressure P = 300 MPa and comparison with experimental data [20]. (♦) n-tridecane, (▲) n-hexadecane, (■) n-octadecane, (●) n-eicosane, (—) prediction.

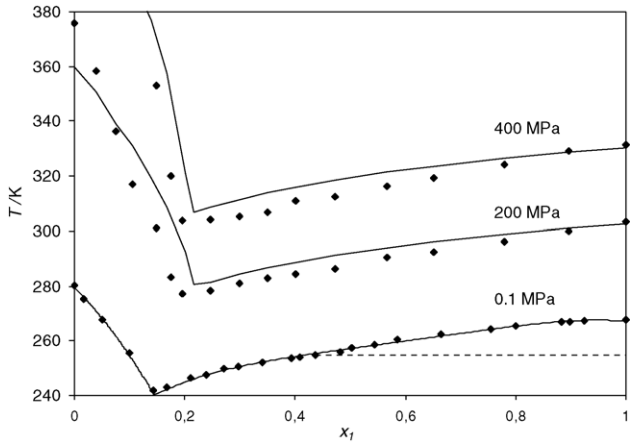

Fig. 4. Prediction of freezing temperatures of {n-tridecane (1) + cyclohexane (2)} system at different pressures P = 200 and 400 MPa and at atmospheric pressure. Solid line at 0.1 MPa describing experimental points are calculated by Wilson equation; dotted line exhibits solid–solid phase transition.

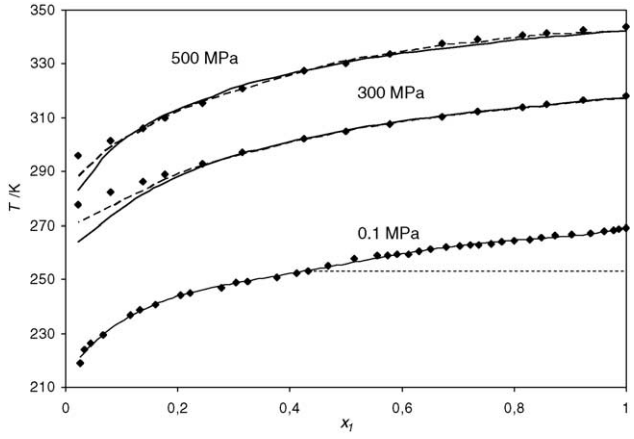

Fig. 5. Freezing temperatures of {n-tridecane (1) + n-hexane (2)} system at different pressures P = 300 and 500 MPa and at atmospheric pressure. Comparison of prediction Eq. (11), (solid line) and correlation with Eq. (14) (dashed line). Dotted line exhibits solid–solid phase transition.

range from x_1 = 0 to 1. The experimental high-pressure SLE results of these binary systems are collected in Tables 3–5 and in Figs. 3–9. The relation between temperature T and pressure p of the SLE at constant x can be satisfactorily described with a simple quadratic equation, so the p–x diagram can be transformed into the T–x diagram. The results are shown in Figs. 3–5. The experimental results shown in Fig. 5 are presented at 300 or 500 MPa and at atmospheric pressure (0.1 MPa).

4. Calculations

4.1. Modelling

The condition of equilibrium between the solid and liquid phases is given by the equality of the fugacities in both phases

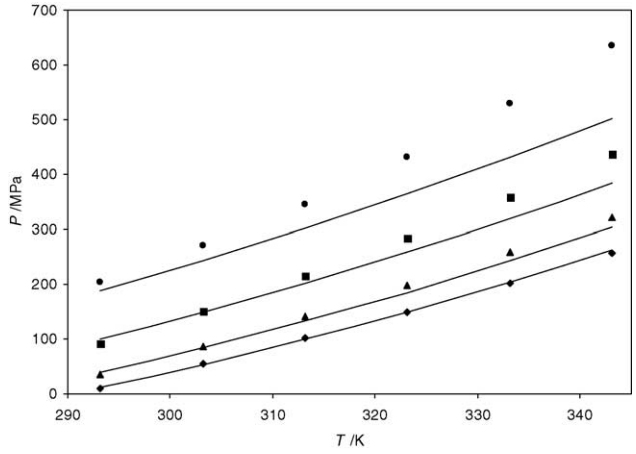

Fig. 6. Experimental data and prediction by Eq. (11) of system {*n*-hexadecane (1) + *n*-hexane (2)} at constant mole fractions. (●) 0.1000; (■) 0.2765; (▲) 0.6002; (♦) 0.9543; solid line (—) prediction.

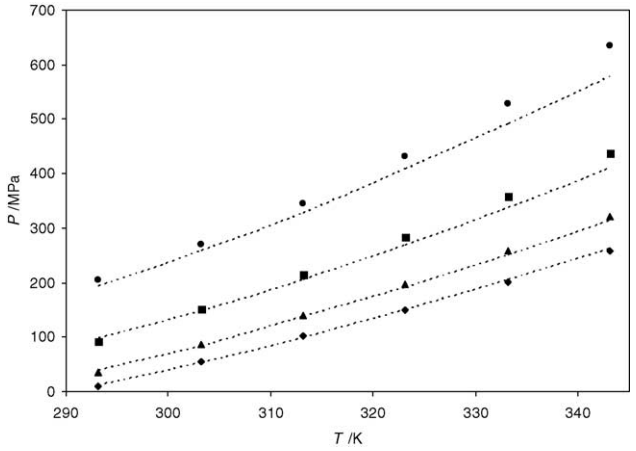

Fig. 7. Experimental data and correlation by the Eq. (14) of system {*n*-hexadecane (1) + *n*-hexane (2)} at constant mole fractions. (●) 0.1000; (■) 0.2765; (▲) 0.6002; (♦) 0.9543; dotted line correlation.

for each individual component, *i*:

$$f_i^{\mathrm{l}}(T, p, x_i^{\mathrm{l}}) = f_i^{\mathrm{s}}(T, p, x_i^{\mathrm{s}}) \tag{1}$$

For the systems studied here the solid phase is a pure compound and the liquid phase is a binary mixture.

The general (solid + liquid) equilibrium (SLE) equation relates, for the crystallizing compound, the fugacities of both phases in the standard state, $f_i(P_0)$, with the pure component thermophysical properties [28]:

$$\ln\frac{f_i^{\mathrm{l}}(P_0)}{f_i^{\mathrm{s}}(P_0)} = \frac{\Delta_{\mathrm{fus}}H_i}{RT_{\mathrm{fus},i}}\left(\frac{T_{\mathrm{fus},i}}{T}-1\right) + \frac{\Delta_{\mathrm{tr}}H_i}{RT_{\mathrm{tr},i}}\left(\frac{T_{\mathrm{tr},i}}{T}-1\right) - \frac{\Delta_{\mathrm{s}}^{\mathrm{l}}Cp_{\mathrm{m}}}{R}\left(\ln\frac{T}{T_{\mathrm{fus},i}} + \frac{T_{\mathrm{fus},i}}{T} - 1\right) \tag{2}$$

Since for the compounds studied in this work only *n*-tridecane presents solid–solid phase transition the second term of Eq. (2) will be used only for systems containing this compound. For the other systems Eq. (2) will be used without its second term. The fugacity of the solid phase at pressure *P* can be obtained through correcting the standard state fugacity with the Poyinting correction:

$$\ln f_i^{\mathrm{s}}(P) = \ln f_i^{\mathrm{s}}(P_0) + \frac{1}{RT}\int_{P_0}^{P} V_i^{\mathrm{s0}}\mathrm{d}P \tag{3}$$

Since no equation of state for the solid phase is available the solid phase molar volume V_i^{s0} will be taken as proportional to the corresponding pure liquid molar volume:

$$V_i^{\mathrm{s0}} = \beta V_i^{\mathrm{l0}} \tag{4}$$

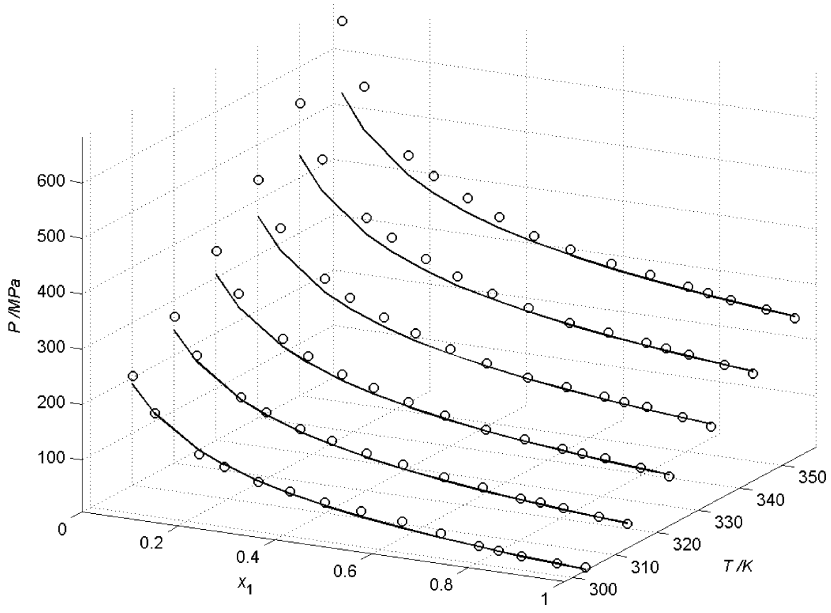

Fig. 8. Prediction and experimental data of {*n*-octadecane (1) + *n*-hexane (2)} system.

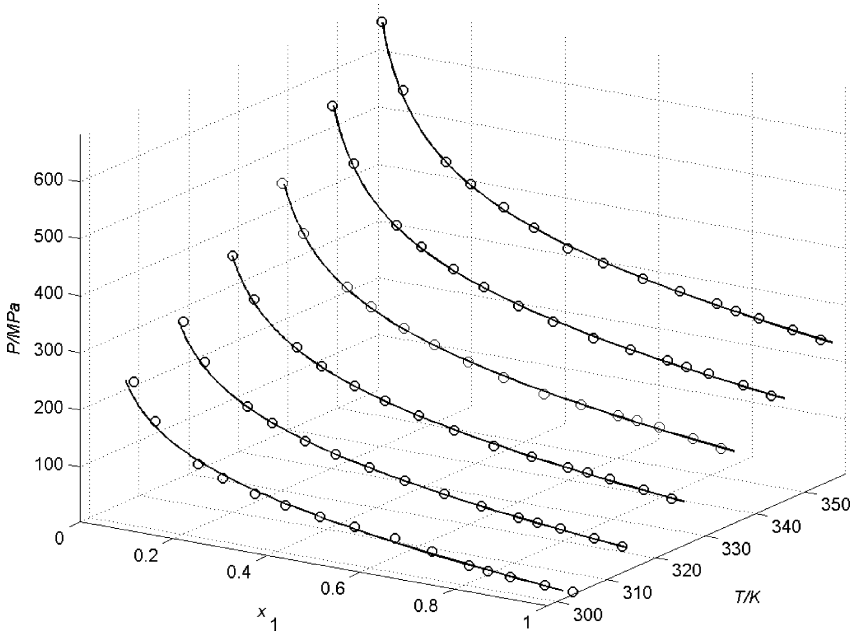

Fig. 9. Correlation by the Eq. (14) and experimental data of {*n*-octadecane (1) + *n*-hexane (2)} system.

In previous works [17,29–32], a constant value of β was used up to 100 MPa with very good results. Preliminary calculations showed that this simplification would not hold above 250 MPa. Since pressures much higher than 250 MPa were used in this work a new approach to estimate β was adopted. Knowing from the experimental measurements that dP/dT is fairly constant for a broad range of pressures, and that the enthalpy of fusion is fairly pressure independent according to some authors [33], it follows from the Clapeyron equation that:

$$T(V_i^{\mathrm{l}} - V_i^{\mathrm{s0}}) = \alpha \tag{5}$$

where α is a constant. Using Eq. (4) a new expression for β is then obtained:

$$\beta = \frac{V_i^{\mathrm{l}}}{V_i^{\mathrm{s0}}} - \frac{\alpha}{TV_i^{\mathrm{l}}} \cong 1 - \frac{\alpha}{TV_i^{\mathrm{l0}}} \tag{6}$$

Note that within this new approach β is still pressure independent and the Poyinting factor is not affected.

The evaluation of liquid fugacities is performed using the Soave–Redlich–Kwong equation of state [34] corrected by the volume translation of Peneloux et al. [35]:

$$P = \frac{RT}{(V' - b)} - \frac{a(T)}{V'(V' + b)} \tag{7}$$

with

$$V_i = V_i' + C_i \tag{8}$$

where V' is the molar volume calculated from the SRK-EOS. C_i is calculated from the GCVOL group contribution method [36] at atmospheric pressure by

$$C_i = V_i^{\mathrm{GCVOL}} - V_i^{\mathrm{EOS}}$$

For mixtures the van der Waals one fluid mixing rules are used:

$$a = \sum_i \sum_j x_i x_j \sqrt{a_i a_j}(1 - k_{ij}) \tag{9}$$

$$b = \sum_i x_i b_i \tag{10}$$

with the k_{ij}'s obtained from the correlation by Jaubert and Mutelet [37].

For crystallizing compounds the equilibrium constant K_i^{s} for the solid phase in a situation of a pure solid phase, is thus given by [18]:

$$K_i^{\mathrm{s}} = \frac{x_i^{\mathrm{s}}}{x_i^{\mathrm{l}}} = \phi_i^{\mathrm{l}}[P](\phi_i^{\mathrm{l0}}[P_0])^{\beta-1}(\phi_i^{\mathrm{l0}}[P])^{-\beta}\left(\frac{P}{P_0}\right)^{1-\beta} \times \exp\left\{\frac{(1-\beta)C_i(P-P_0)}{RT} + \frac{\Delta_{\mathrm{fus}}H_i}{RT_{\mathrm{fus},i}}\left(\frac{T_{\mathrm{fus},i}}{T} - 1\right) + \frac{\Delta_{\mathrm{tr}}H_i}{RT_{\mathrm{tr},i}}\left(\frac{T_{\mathrm{tr},i}}{T} - 1\right) - \frac{\Delta_{\mathrm{s}}^{\mathrm{l}}Cp_{\mathrm{m}}}{R}\left(\ln\frac{T}{T_{\mathrm{fus},i}} + \frac{T_{\mathrm{fus},i}}{T} - 1\right)\right\} \tag{11}$$

with the liquid phase fugacity coefficients, ϕ_i^{l} calculated from the equation of state. P_0 is the reference pressure, taken as atmospheric pressure.

4.2. Correlation

A SLE correlation method was proposed based on Eq. (2) [11,20]. It was showed that the activity coefficient γ_1 at

higher pressure could be expressed as:

$$\ln \gamma_1 = \sum_{i=0}^{3} a_i \left(\frac{1}{T} - \frac{1}{T_{\mathrm{fus},1}} \right)^i + a' \left(\ln \frac{T}{T_{\mathrm{fus},1}} + \frac{T_{\mathrm{fus},1}}{T} - 1 \right) \quad (12)$$

and after substituting Eq. (12) into Eq. (2) for binary systems and simplifications we obtain:

$$\ln x_1 = \sum_{i=0}^{3} b_i \left(\frac{1}{T} - \frac{1}{T_{\mathrm{fus},1}} \right)^i + b' \left(\ln \frac{T}{T_{\mathrm{fus},1}} + \frac{T_{\mathrm{fus},1}}{T} - 1 \right) \quad (13)$$

where $b_0 = -a_0$, $b_1 = -a_1 - \Delta_{\mathrm{fus}} H_1/R$, $b_2 = -a_2$, $b_3 = -a_3$, $b' = -a' + \Delta_1^{\mathrm{s}} C p_{\mathrm{m},1}/R$.

The value of the second term on the right hand side of Eq. (13) is small and this term can be neglected. Thus, the Eq. (13) may be rewritten in a simple form:

$$\ln x_1 = \sum_{i=0}^{3} b_i \left(\frac{1}{T} - \frac{1}{T_{\mathrm{fus},1}} \right)^i \quad (14)$$

(Solid + liquid) equilibrium curves are dependent on pressure. With increasing pressure the SLE curves shift to higher temperatures. In Eq. (14), the b_i terms were found to be pressure-dependent and which dependence can be expressed as follows:

$$b_i = \sum_{j=0}^{2} D_{ji} P^j \quad (15)$$

The objection function O.F., used in the fit of the parameters of the Eqs. (14) and (15) was:

$$\mathrm{O.F.} = \sum_{i=1}^{n} \omega_i^{-2} (\ln x_{1i}^{\mathrm{cal.}}(T_i, P_i, D_{ji}) - \ln x_{1i}) \quad (16)$$

where $\ln x_{1i}^{\mathrm{cal.}}$ denotes values of the logarithm of the solute mole fraction calculated from the Eq. (14), $\ln x_{1i}$ denotes the logarithm of the experimental solute mole fraction and the symbols, T_i, P_i, D_{ji} express temperature, pressure and coefficients from Eq. (15), respectively; ω_i is the weight of the calculated values, described by means of the error propagation formula. Eq. (14) is a fitting routine giving a large number of parameters D_{ji}, which are characteristic for the binary mixtures. These parameters describe the influence of high pressure on the system and the deviations given by the simple thermodynamic model. Table 6 contains the coefficients D_{ji} from Eq. (15) for the measured systems. Experimental points correlated with Eq. (14) at constant pressure are shown in Figs. 5, 7 and 9. The solid lines in Fig. 5 represent the predictions, dashed lines correlation with Eq. (14). The values of standard mean deviation of correlation in $\ln x_1$ are from 1.6 to 4.8×10^{-2}. Calculated solidus curves are in good agreement with the experimental data. The comparison of the values of the average standard mean deviation in T and P are collected in Table 7. Standard deviations of prediction are two or more times higher than standard deviations of correlation because prediction shows slight deviations from the experimental data in the area of eutectic conditions.

Table 6
Parameters D_{ji} of Eq. (15) for investigated {*n*-alkane (1) + *n*-hexane (2)} systems

	n-Tridecane	*n*-Hexadecane	*n*-Octadecane
D_{00}	-1.1858	-1.1555×10^{-1}	7.9436×10^{-3}
D_{10}	3.3231×10^{-3}	-1.0407×10^{-2}	-1.3580×10^{-2}
D_{20}	-3.0972×10^{-5}	-8.4178×10^{-6}	-1.0643×10^{-6}
D_{01}	-7.4718×10^{3}	-4.3366×10^{3}	-4.0584×10^{3}
D_{11}	3.8441×10^{1}	1.3727×10^{1}	-1.2842×10^{1}
D_{21}	-1.0775×10^{-1}	-9.5197×10^{-2}	-3.4083×10^{-2}
D_{02}	-6.7662×10^{6}	3.6524×10^{6}	3.5113×10^{6}
D_{12}	4.6942×10^{4}	1.1414×10^{4}	-6.4523×10^{4}
D_{22}	-1.1264×10^{2}	-1.3213×10^{2}	2.2421×10^{1}
D_{03}	-7.0707×10^{9}	-1.2897×10^{9}	-1.2440×10^{10}
D_{13}	2.6171×10^{7}	3.5236×10^{6}	-1.7648×10^{7}
D_{23}	-4.1658×10^{4}	-2.5010×10^{4}	3.6300×10^{4}
σ[a]	0.0160	0.0483	0.0224

[a] The standard deviation $\sigma = \left(\sum_{i=1}^{n} (\ln x_i^{\mathrm{cal.}} - \ln x_i)^2/(n-12) \right)^{1/2}$.

The values of α of Eq. (5) [32] were fitted to the pure compounds melting temperatures for a wide range of pressures. As expected the value is related to solid phase crystalline behaviour. A common value of $\alpha = 0.060\ \mathrm{K\ dm^3\ g^{-1}}$ was obtained for the even *n*-alkanes. Values, 0.043 and $0.018\ \mathrm{K\ dm^3\ g^{-1}}$ were used for *n*-tridecane and cyclohexane, respectively. While for *n*-alkanes the heat capacity term in Eqs. (1) and (11) is generally negligible, it was found that for cyclohexane, due to its low enthalpy of melting, the inclusion of this term improves the description of the data. To keep a purely predictive approach for mixtures, the k_{ij}'s were estimated from a group contribution model [37] and identical k_{ij}'s were used for both the hexane and cyclohexane solvents. The results of the predictions for systems with cyclohexane are presented in Figs. 3 and 4. Comparison of correlation and prediction is shown for the system (*n*-tridecane + *n*-hexane) in Fig. 5; for systems (*n*-hexadecane + *n*-hexane) and

Table 7
Comparison of prediction and correlation: the average standard deviations in temperature T and pressure P in all measured systems

System	EOS – G^{E}		Correlation	
	σ_T[a] (K)	σ_P[b] (MPa)	σ_T[a] (K)	σ_P[b] (MPa)
n-Tridecane + *n*-hexane	1.78	28.82	1.17	17.23
n-Tridecane + cyclohexane	10.03	52.65	2.69	21.46
n-Hexadecane + *n*-hexane	3.84	27.49	2.74	13.63
n-Hexadecane + cyclohexane	6.12	33.40	0.29	1.79
n-Octadecane + *n*-hexane	1.52	15.46	0.86	6.92
n-Octadecane + cyclohexane	4.33	24.48	0.27	1.72
n-Eicosane + cyclohexane	5.95	34.15	2.59	12.38

[a] The standard deviation $\sigma_T = \left(\sum_{i=1}^{n} (T_i^{\mathrm{cal.}} - T_i)^2/n \right)^{1/2}$.

[b] The standard deviation $\sigma_P = \left(\sum_{i=1}^{n} (P_i^{\mathrm{cal.}} - P_i)^2/n \right)^{1/2}$.

(*n*-octadecane + *n*-hexane) in Figs. 6 and 7 or in Figs. 8 and 9, separately, for prediction and correlation. The description of the experimental data is quite good in particular if one takes into account that the model used is purely predictive, only pure component data are used to predict the mixture behaviour and the pressures are extremely large, far above the pressure range in which cubic equations of state are normally applied.

The limitations in the description close to the eutectic point must be related to a variation of the volume of phase change, (V^l–V^s), with pressure [38], which will make the β parameter pressure-dependent. This cannot be considered within the framework of the adopted model. Such dependence is not apparent for the *n*-alkanes, where the larger value of α makes them less sensitive to pressure effects.

Sometimes, an inflection point on the liquidus was observed, which is characteristic for a solid–solid phase transition as discussed for (*n*-alkane + ether) mixtures [21]. According to literature data [22], at normal pressure only *n*-tridecane and *n*-eicosane show a solid–solid first order transition close to the melting point. The literature review of Dirand et al. [22], discusses the existence of solid–solid transitions, observed by DSC studies and X-ray diffraction, but does not present the values of the enthalpy of phase transition. Solid–solid phase transitions may be present in the case of high purity *n*-octadecane and *n*-eicosane at atmospheric pressure. For *n*-tridecane the rotational transition is observed up to 300 MPa when the transition and melting points converge [39]. This phase behavior of *n*-tridecane is typical for all investigated odd *n*-alkanes. For higher even *n*-alkanes C_{20}–C_{30} [33] and C_{22}–C_{30} [40] the distance between the transition and fusion temperature decreases with increasing pressure. Only a slight increase of 10% was observed in the sum of enthalpies changes of solid–solid phase transition and fusion with increasing pressure up to 300 MPa [40]. Unfortunately, from the results presented in this work (see Figs. 4 and 5) it is not easy to find new information on the solid–solid phase transition type $\alpha \rightarrow \beta$ and on the influence of pressure on the transition temperatures.

5. Conclusions

(Solid + liquid) phase equilibria for three systems of binary (*n*-alkane + *n*-hexane) mixtures have been investigated at pressures up to 1.0 GPa. The freezing curves shift monotonously to higher temperatures with increasing pressure. A new method of prediction of (solid + liquid) equilibria at pressures higher than 300 MPa is presented. Seven systems with (*n*-alkanes + cyclohexane, or *n*-hexane) were tested with new model and the accuracy was very good excluding compositions close to eutectic points. If one takes into account that the proposed model uses only pure component data to predict binary mixture behavior, the results seem to be very satisfactory. The proposed model can thus be very useful for practical purposes.

For systems of *n*-alkanes with *n*-hexane the correlation equation, proposed by Yang et al. [10,11] was used with very good results. It occurred, that the higher pressure makes larger deviations in the description of the (solid + liquid) equilibria and for these purposes a more flexible equation was necessary to use, which was previously proposed to the (1-alkanol + *n*-hydrocarbon) binary systems [11].

Acknowledgement

The authors gratefully acknowledge the Warsaw University of Technology for the financial support.

References

[1] B. Baranowski, Polish J. Chem. 52 (1978) 1789–1801.
[2] B. Baranowski, A. Moroz, Polish J. Chem. 56 (1982) 379–391.
[3] D. Dudek, B. Baranowski, Polish J. Chem. 65 (1991) 1357–1366.
[4] D. Dudek, B. Baranowski, Polish J. Chem. 68 (1994) 1267–1291.
[5] K. Nagaoka, T. Makita, Int. J. Thermophys. 9 (1998) 61–71.
[6] K. Nagaoka, T. Makita, Int. J. Thermophys. 9 (1988) 535–545.
[7] K. Nagaoka, T. Makita, Int. J. Thermophys. 8 (1987) 671–680.
[8] K. Nagaoka, T. Makita, N. Nishiguchi, M. Moritoki, Int. J. Thermophys. 10 (1989) 27–34.
[9] Y. Tanaka, M. Kawakami, Fluid Phase Equilib. 125 (1996) 103–114.
[10] M. Yang, E. Terakawa, Y. Tanaka, T. Sotani, S. Matsuo, Fluid Phase Equilib. 194–197 (2002) 1119–1129.
[11] M. Yang, T. Narita, Y. Tanaka, T. Sotani, S. Matsuo, Fluid Phase Equilib. 204 (2003) 55–64.
[12] T. Inoue, I. Motoda, N. Hiramatsu, M. Suzuki, K. Sato, Chem. Phys. Lipids 82 (1996) 63–72.
[13] J.A.P. Coutinho, S.I. Andersen, E.H. Stenby, Fluid Phase Equilib. 117 (1996) 138–145.
[14] P. Hemmingsen, Doctoral Thesis, Department of Chem. Eng., Norwegian University of Science and Technology, Norway, 2000.
[15] G. Sadowski, W. Arlt, A. De Haan, G. Krooshof, Fluid Phase Equilib. 163 (1999) 79–87.
[16] T. Tork, C. Yokoyama, S. Moriya, T. Ebina, Sekiyu Gakkaishi-J. Jpn. Petrol. Inst. 41 (1998) 125–135.
[17] J. Pauly, J.-L. Daridon, J.A.P. Coutinho, N. Lindeloff, S.I. Andersen, Fluid Phase Equilib. 167 (2000) 145–159.
[18] J. Pauly, J.-L. Daridon, J.A.P. Coutinho, Fluid Phase Equilib. 187–188 (2001) 71–82.
[19] S.J. Sawamura, Solution Chem. 29 (2000) 369–375.
[20] U. Domańska, P. Morawski, Fluid Phase Equilib. 218 (2004) 57–68.
[21] U. Domańska, P. Morawski, Phys. Chem. Chem. Phys. 4 (2002) 2264–2268.
[22] M. Dirand, M. Bouroukba, A.-J. Briard, V. Chevallier, D. Petitjean, J.-P. Corriou, J. Chem. Thermodyn. 34 (2002) 1255–1277.
[23] M. Palczewska-Tulińska, D. Wyrzykowska-Stankiewicz, A.M. Szafrański, J. Choliński, Solid And Liquid Heat Capacity Data Collection, part 2: C6–C33, DECHEMA e.V. Germany, 1997, p. 4.
[24] U. Domańska, P. Morawski, J. Chem. Thermodyn. 33 (2001) 1215–1226.
[25] U. Domańska, K. Kniaż, Int. DATA Ser., Ser. A, Sel. DATA Mix. 2 (1990) 83–92.
[26] U. Domańska, J. Rolińska, A.M. Szafrański, Int. DATA Ser., Ser. A, Sel. DATA Mix. 4 (1987) 270.
[27] A.R. Ubbelonde, The Molten State of Matter, in: Melting and Crystal Structure, John Willey & Sons, Chichester, New York, Brisbane, Toronto, 1978, p. 14.

[28] M. Prausnitz, R.N. Lichtenthaler, E.G. Azevedo, E.G. Molecular, Thermodynamics of Fluid-Phase Equilibria, third ed., Prentice-Hall, Upper Saddle River, NJ, 1999.
[29] J.J. Pauly, J.-L. Daridon, J.A.P. Coutinho, F. Montel, Energy Fuels 15 (2001) 730–735.
[30] J. Pauly, J.-L. Daridon, J.M. Sansot, J.A.P. Coutinho, Fuel 82 (2003) 595–601.
[31] J.M. Sansot, J. Pauly, J.A.P Coutinho, J.-L. Daridon, AIChE J., 2004, submitted for publication.
[32] J. Pauly, J.-L. Daridon, J.A.P. Coutinho, Fuel, 2004, submitted for publication.
[33] G.W.H. Höhne, K. Blankenhorn, Thermochim. Acta 238 (1994) 351–370.
[34] G. Soave, Chem. Eng. Sci. 27 (1972) 1197–1203.
[35] A. Peneloux, E. Rauzy, R. Frèze, Fluid Phase Equilib. 8 (1982) 7–23.
[36] H.S. Elbro, A. Fredenslund, P. Rasmussen, Ind. Eng. Chem. Res. 30 (1991) 2576–2582.
[37] J.N. Jaubert, F. Mutelet, Fluid Phase Equilib. 224 (2004) 285–304.
[38] K.D. Wisotzki, A. Wurflinger, J. Phys. Chem. Solids 43 (1982) 13–20.
[39] A. Würflinger, G.M. Schneider, Ber. Bunsenges. 77 (1973) 121–128.
[40] Ch. Nakafuku, T. Sugiuchi, Polymer 34 (1993) 4945–4952.